Underwater noise comparison of pre- and post-retrofitted MAERSK G-class container vessels

Martin Gassmann, Lee B. Kindberg, Sean M. Wiggins and John A. Hildebrand

Marine Physical Laboratory
Scripps Institution of Oceanography
University of California San Diego
La Jolla, California 92093-0205
martin.gassmann044@gmail.com

MPL TM-616
October 2017

Contents

Executive Summary

As part of a radical retrofit program, MAERSK LINE, the world's largest container shipping company, has modified eleven G-class container vessels in the years of 2015 and 2016 under an investigative and energy-efficiency improvement effort. As the radical retrofit includes replacing the bulbous bow to reduce drag, derating the main engines for slow steaming and installing more efficient propellers with propeller boss cap fins to reduce cavitation, another benefit of the retrofit may be reduction in underwater radiated noise.

The Marine Physical Laboratory at the Scripps Institution of Oceanography has opportunistically recorded underwater noise radiated by commercial vessels, including MAERSK G-class vessels before and after their retrofits, as they transit from the ports of Los Angeles (POLA) and Long Beach (POLB) in the northbound shipping lane through the Santa Barbara Channel off the coast of California. Five MAERSK G-class vessels, GRETE, GUDRUN, GUNVOR, GERDA and GERNER, were selected to compare the underwater radiated noise before and after the vessels' radical retrofits, utilizing a total of 36 transits at speeds between 4 m/s and 11 m/s.

The estimated underwater source sound pressure levels of the five selected MAERSK G-class vessels were found to be lower for post-retrofitted vessels by a median of 6 dB in the low-frequency band (8 - 100 Hz) and a median of 8 dB in the high-frequency band (100 - 1000 Hz), when compared to pre-retrofitted vessel estimated source sound pressure levels. The reduction in source sound pressure levels, in particular in the low-frequency band, may result from less cavitation due to both the retrofitted propellers with boss cap fins, and to propeller operation at greater depth where ambient pressure is higher.

Reductions of ship source sound pressure level due to changes such as those employed by the radical retrofits may result in ocean-basin-wide noise reductions.

Background

Underwater noise from shipping is a significant contributor to low-frequency ambient noise (<100 Hz) in the ocean (Wenz, 1962; Hildebrand, 2009). It is unintentionally generated by the ships' movement through the water and by the ships' auxiliary and propulsion machineries, in particular propellers (Urick, 1975; Ross, 1976). The cavitation processes occurring near the tip of rotating propellers generate underwater noise over a broad frequency range and at a series of distinct frequencies that is related to the propeller blade rate and therefore to a ship's speed (Gray and Greeley, 1980). Ships that operate at higher speeds have been observed to radiate underwater noise at a higher intensity into the marine environment (Jansen and de Jong, 2015; Simard *et al.*, 2016).

Various animals in marine environments, such as whales and dolphins, rely on underwater sound to navigate, feed and communicate. Given the high intensity of ship underwater radiated noise and its low-frequency, long-range propagation, environmental concerns about noise contributions from commercial shipping have been raised at both, the regional and the global level, e.g. (Erbe *et al.*, 2012; Redfern *et al.*, 2017).

As the global seaborne trade has doubled over the last couple of decades with a volume of over 10 billion tons in the year of 2015 alone, the world commercial shipping fleet has grown dramatically (UNCTAD, 2016) . As of January 1st, 2016, the world commercial fleet consisted of 90,917 vessels in total with a combined capacity of 1.8 billion deadweight tonnage (DWT). Vessels for containerized cargo, referred to as container vessels, have concurrently not only increased in number, but also in their cargo capacity and as a result have become significantly larger. While a larger container vessel may require for the same amount of cargo less transits than a smaller container vessel, larger container vessels, however, have been observed to radiate underwater noise during their transits at a higher intensity into the marine environment, as more energy is needed for their operation (McKenna *et al.*, 2013).

The world's largest container shipping company, MAERSK LINE, has been investing significantly to investigate and improve the energy efficiency and greenhouse gas emissions performance of its fleet (MAERSK LINE, 2017). As part of this work, eleven out of twelve MAERSK G-class container vessels underwent a $100+ million Radical Retrofit Program. This includes replacing the bulbous bow to reduce drag, derating the main engines for slow steaming and installing more efficient, four-bladed propellers with propeller boss cap fins to reduce cavitation, which may also reduce the underwater noise radiated by retrofitted MAERSK G-class vessels during their operation (Figure 1).

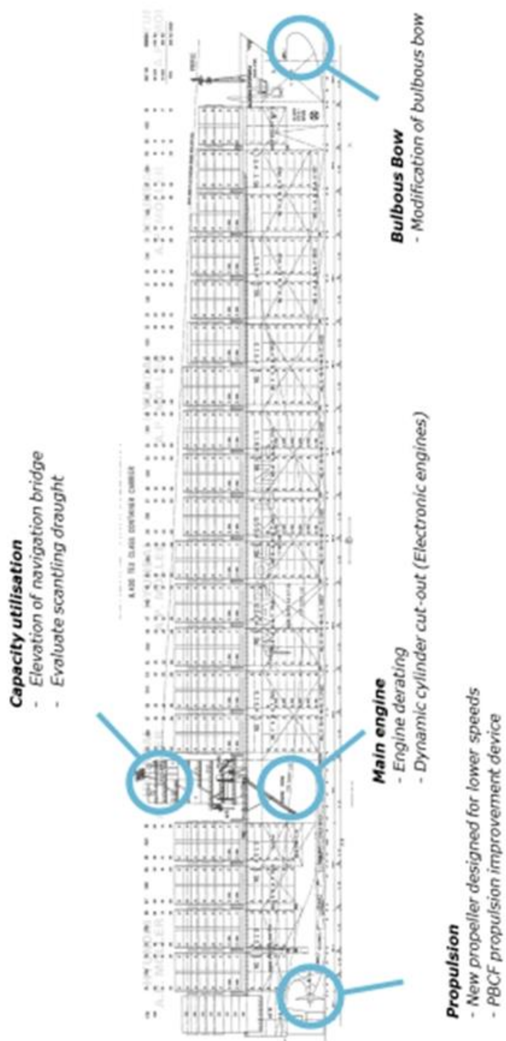

Figure 1 Components of Radical Retrofit applied to MAERSK G-class vessels

The goal of the Radical Retrofit Program is to reduce fuel consumption through increased efficiency and to increase cargo capacity by over 1,000 twenty-foot-equivalent units (TEU). These vessels are also now part of a Technology Advancement Project funded by the Ports of Los Angeles and Long Beach which will relate these efficiency improvements to air emissions and greenhouse gases.

The Marine Physical Laboratory at the Scripps Institution of Oceanography has made opportunistic recordings of underwater noise radiated by commercial vessels, including MAERSK G-class vessels before and after their retrofits, as they transit from the ports of Los Angeles (POLA) and Long Beach (POLB) in a shipping lane through the Santa Barbara Channel off the coast of California. To compare the underwater radiated noise before and after the vessels' radical retrofits, five MAERSK G-class vessels that were retrofitted in 2015 and 2016 were selected: GRETE MAERSK, GUDRUN MAERSK, GUNVOR MAERSK, GERDA MAERSK and GERNER MAERSK (Table 1).

Table 1 MAERSK G-class vessels selected for analysis.

Vessel IMO	2015 VSL Vessel Name	Vessel Class	Keel Laid Date	Radical Retrofit Completion Date
9359052	GERDA MAERSK	L-211	02-Sep-2008	06-Mar-2016
9359002	GERNER MAERSK	L-211	20-Oct-2007	02-Jul-2016
9302889	GRETE MAERSK	L-197	05-Nov-2004	05-Sep-2015
9302877	GUDRUN MAERSK	L-197	10-Dec-2004	14-Aug-2015
9302891	GUNVOR MAERSK	L-197	01-Jan-2005	08-Oct-2015

Methods

Experimental Setup

Long-term recordings of underwater sound pressure levels were made near shipping lanes off the coast of California in the Santa Barbara Channel by the Marine Physical Laboratory at the Scripps Institution of Oceanography since 2008 (McKenna *et al.*, 2012a; McKenna *et al.*, 2012b) (Figure 2). For the last nine years, underwater sound was recorded by a High-frequency

Acoustic Recording Package (HARP) at a sampling frequency of 200 kHz with a single hydrophone approximately 20 m above the seafloor at 565 m water depth (Wiggins and Hildebrand, 2007). The HARP was deployed (34° 16.53 N 120° 1.11 W) 3 - 4 km north from the center of the 1 nm (1.852 km) wide northbound shipping lane for merchant ships that transit from the POLA and POLB through the Santa Barbara Channel (Figure 2).

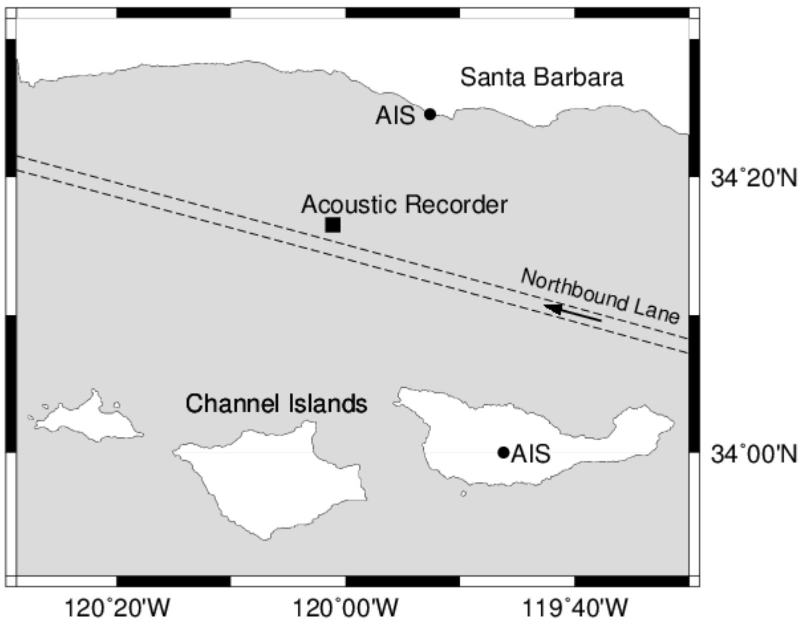

Figure 2 Map of the Santa Barbara Channel showing the locations of the underwater acoustic recorder (square) and the AIS receivers (circles). Dashed lines represent shipping lane with arrow indicating the direction of travel.

Vessel Identification and Tracking

To identify and track MAERSK G-class vessels that transit by the HARP in the northbound shipping lane, position, speed, and vessel data from the Automatic Identification System (AIS) were collected. AIS receivers were located on Santa Cruz Island (33° 59.6670 N and 119° 37.9410 W) and Coal Oil Point (34° 2 4.5320 N 119° 52.68216 W) to provide coverage for the northbound shipping lane and its vicinity (Figure 2). The received AIS messages were time-stamped and continuously logged on-site by a computer. AIS messages were decoded with the Shipplotter program (ver. 12.4.6.5 COAA) and software developed by Robin T. Bye (Project: Virtual More) to search for messages from MAERSK G-class vessels that contain position (latitude and longitude), ship's reference point for the reported position and Speed Over Ground (SOG). These messages were then filtered to retain only messages with positions that were less than 30 km away from the HARP. As the AIS messages were received typically every 10 – 20 s during which the ship speed was presumed to be linearly changing, the positions and SOGs of the filtered AIS messages were linearly interpolated to yield an AIS-derived track with a time resolution of 3 s for any of the transits of the five MAERSK G-class vessels.

Acoustic Data Processing

The timing information of the AIS-derived tracks was used to identify transits of the selected MAERSK G-class vessels in the HARP acoustic recordings. Each identified acoustic record containing the underwater radiated noise from a transiting MAERSK G-class vessel was then downsampled by factor of 20 to yield a Nyquist frequency of 5 kHz. This provides computational savings as the underwater radiated ship noise is mostly absent at frequencies greater than 5 kHz. The downsampled record was then manually examined for corruption from electronic noise and interference from other ships or marine mammals to exclude corrupted records from further processing. To minimize the number of excluded records, the lower and upper limit of the frequency range of interest was set to 8 Hz and 1 kHz, respectively. Start time and length of each record were determined from the time of the closest point of approach (CPA) of the ship's bow and the duration for the ship to travel its own length (35 - 90 sec for SOGs between 11 and 4 m/s), respectively.

Received Sound Pressure Levels

Each of the selected, downsampled acoustic records was divided into consecutive, non-overlapping segments with a length of 1 s (10,000 samples). A two-sided Fast Fourier Transform (FFT) with 10,000 points (NFFT) was applied to each segment to provide a frequency bin spacing of 1 Hz. The magnitude squared values of the complex FFT coefficients for the positive frequencies were multiplied by $2/NFFT^2$ to account for the processing gain of the FFT. Their mean was computed for each frequency bin, $|\overline{FFT}|^2$, and then converted onto a relative logarithmic scale in decibels (dB) with a reference pressure of 1 μPa^2. This quantity is the received sound pressure level (RL):

$$RL = 10log_{10}\left(\frac{|\overline{FFT}|^2}{(1\mu Pa)^2}\right)$$

The frequency distribution of RL will be referred to as RL spectrum and will be shown for 1 Hz bands and for one-third-octave (OTO) bands.

Source Sound Pressure Levels

The source sound pressure level (SL) of underwater radiated noise of each of the five MAERSK G-class vessels was estimated at a reference distance of 1 m using the RL at the HARP and by accounting for the loss in sound transmission (TL) during each transit:

$$SL = RL + TL$$

The TL between the radiating ship and the receiving hydrophone of the HARP was computed with a Lloyd's mirror model to account for the losses caused by interference from surface reflections that are significant for sources at near-surface depths (Gassmann *et al.*, 2017). For this model, the complex horizontal and vertical source distribution of a ship is reduced to a single point source with an effective source depth. The effective source depth of the ship during each transit was computed from her draft measured at her aft minus 85% of her propeller diameter (Gray and Greeley, 1980). Pre- and post-retrofit propeller diameters for all MAERSK G-class vessels were 9 m and 9.3 m, respectively. Propeller offset from the keel line was assumed to be negligible. In addition, slant ranges from the locations of the ship's propeller to the hydrophone of the HARP were computed for the Lloyd's mirror model.

Drafts and slant ranges for the transits of the selected MAERSK G-class vessels that were used in the Lloyd's mirror model are shown for the years 2011-2017 in Figure 3. All drafts of the post-retrofitted MAERSK G-class vessels were greater than 12 m while drafts of the pre-retrofitted vessels were shallower between 9 – 12 m, except for one pre-retrofit transit of GRETE and GERNER (upper panel in Figure 3). This is presumably due to the increased cargo capacity of the retrofitted MAERSK G-class vessel by over 1,000 twenty-foot equivalent units (TEU), which causes the retrofitted vessels to travel with a greater draft. Slant ranges varied between 3.4 and

5 km (center panel in Figure 3), presumably due to the course chosen by the MAERSK G-class vessels in the 1.852 km wide shipping lane. No significant difference in slant range between pre- and post-retrofit transits was found. Furthermore, SOGs varied by transit between 4 – 11 m/s with all post-retrofit SOGs below 8 m/s (lower panel in Figure 3).

The frequency distribution of SL will be referred to as SL spectrum and will be shown for 1 Hz bands and for one-third-octave (OTO) bands.

Determination of Differences in Received Sound Pressure Levels and in Source Sound Pressure Levels due to Retrofitting

To distinguish between noise radiated by the propeller and by other ship machinery such as generators, the frequency range of interest (8 - 1000 Hz) was divided into low (8 - 100 Hz) and high (100- 1000 Hz) frequency bands. For each band and transit, a one RL and one SL value was computed by integrating over the magnitude-squared pressure values of the respective band. The lower limit of 8 Hz was selected to minimize the impact of pressure fluctuations due to ocean waves on the recorded signal (Webb, 1998).

The SOG-dependent RL and SL distributions for the low- and high-frequency band were divided further into pre- and post-retrofit sub-distributions resulting into four RL and four SL sub-distributions. First-order polynomials were fitted to each of the eight SOG-dependent sub-distributions by using a Theil-Sen robust linear regression algorithm (Gilbert, 1987) as a means for predicting the contribution of ship speed to the radiated noise.

The first-order polynomials fitted to the pre-retrofit distributions establish the pre-retrofit base lines for RL and SL in the low- and high-frequency band. Differences between these pre-retrofit base lines and the post-retrofit distributions were computed and charted as histograms with a bin size of 2 dB to evaluate changes in received and source sound pressure levels due to retrofitting. To characterize the goodness of fit of the first-order polynomials for the pre-retrofit base lines, differences between the pre-retrofit base lines and the pre-retrofit distributions were computed and charted also as histograms with a bin size of 2 dB.

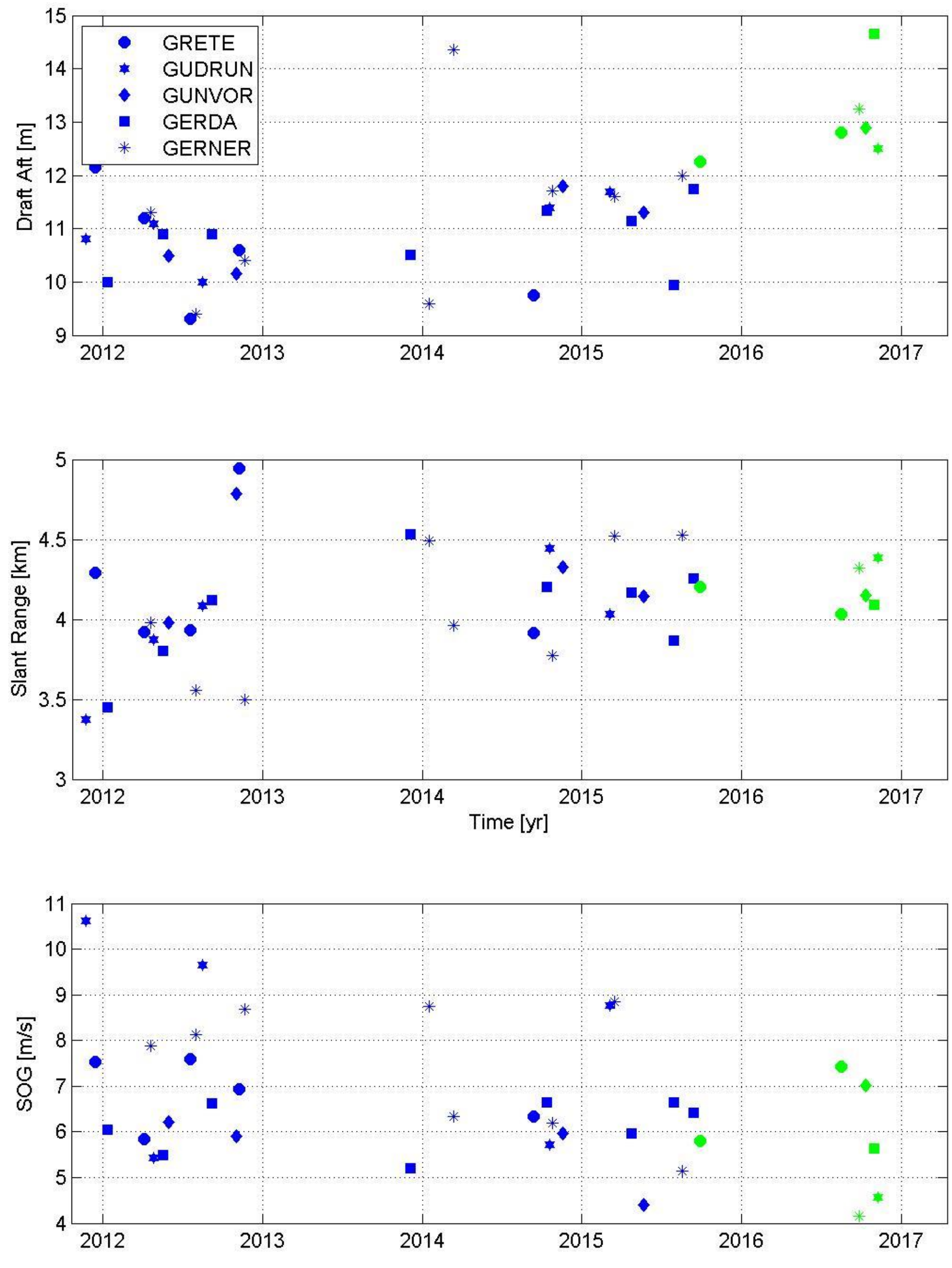

Figure 3 Draft, speed (SOG,) and slant range at the closest point of approach to the acoustic recorder for transits of GRETE (circles), GUDRUN (hexagrans), GUNVOR (diamonds), GERDA (squares) and GERNER (stars) between December 2011 and November 2016. Pre- and post-retrofit values are represented by blue and green symbols, respectively.

Results

A total of 36 transits of the five selected MAERSK G-class vessels were used to compute RL and SL spectra. To exemplify the dependence on speed and differences due to retrofitting, RL and SL spectra of three transits from the GUDRUN MAERSK are shown in Figure 4. For the transit at low speed (5.7 m/s), the values of the RL spectrum are generally lowest (red line, upper panel in Figure 4). Values of the RL spectrum for the high-speed, post-retrofit transit (9.3 m/s) are similar for frequencies smaller than 100 Hz or lower for frequencies greater than 100 Hz than for the high-speed, pre-retrofit transit (9.7 m/s) (upper panel in Figure 4). In contrast, the values of the SL spectrum for the high-speed, post-retrofit transit are generally lower than for the high-speed, pre-retrofit transit while being greater or similar than for the low-speed transit (lower panel in Figure 4). A complete presentation of the RL and SL spectra from all transits in 1 Hz and one-third octave (OTO) bands can be found in Appendix A.

Pre- and post-retrofit RL and SL distributions along with the fitted, speed-dependent baselines are shown for the low-frequency (8 - 100 Hz) and high-frequency (100 - 1000 Hz) band in Figure 5 and Figure 6, respectively**.** For the dominant low-frequency band, there are no significant differences between the pre- and post-retrofit RL distribution yielding a maximum difference between the pre- and post-retrofit baselines of less than 1 dB (upper panel in Figure 5). In contrast, the baseline for the post-retrofit SL distribution is significantly lower than for the pre-retrofit SL distribution by 3 – 8 dB, depending on vessel speed (lower panel in Figure 5). SLs for the post-retrofitted vessels range from 188 dB re 1µPa m (8-100Hz) at a SOG of 4.4 m/s to 205 dB re 1µPa m (8-100Hz) at a SOG of 9.3 m/s while SLs for pre-retrofitted vessels ranged from 190 dB re 1µPa m (8-100Hz) at 4.5 m/s to 214 dB re 1µPa m (8-100Hz) at 10.6 m/s. For the high-frequency band, the baselines for the post-retrofit RL and SL distribution are both lower by 1-3 dB and 6 – 9 dB than their respective pre-retrofit baselines (Figure 6).

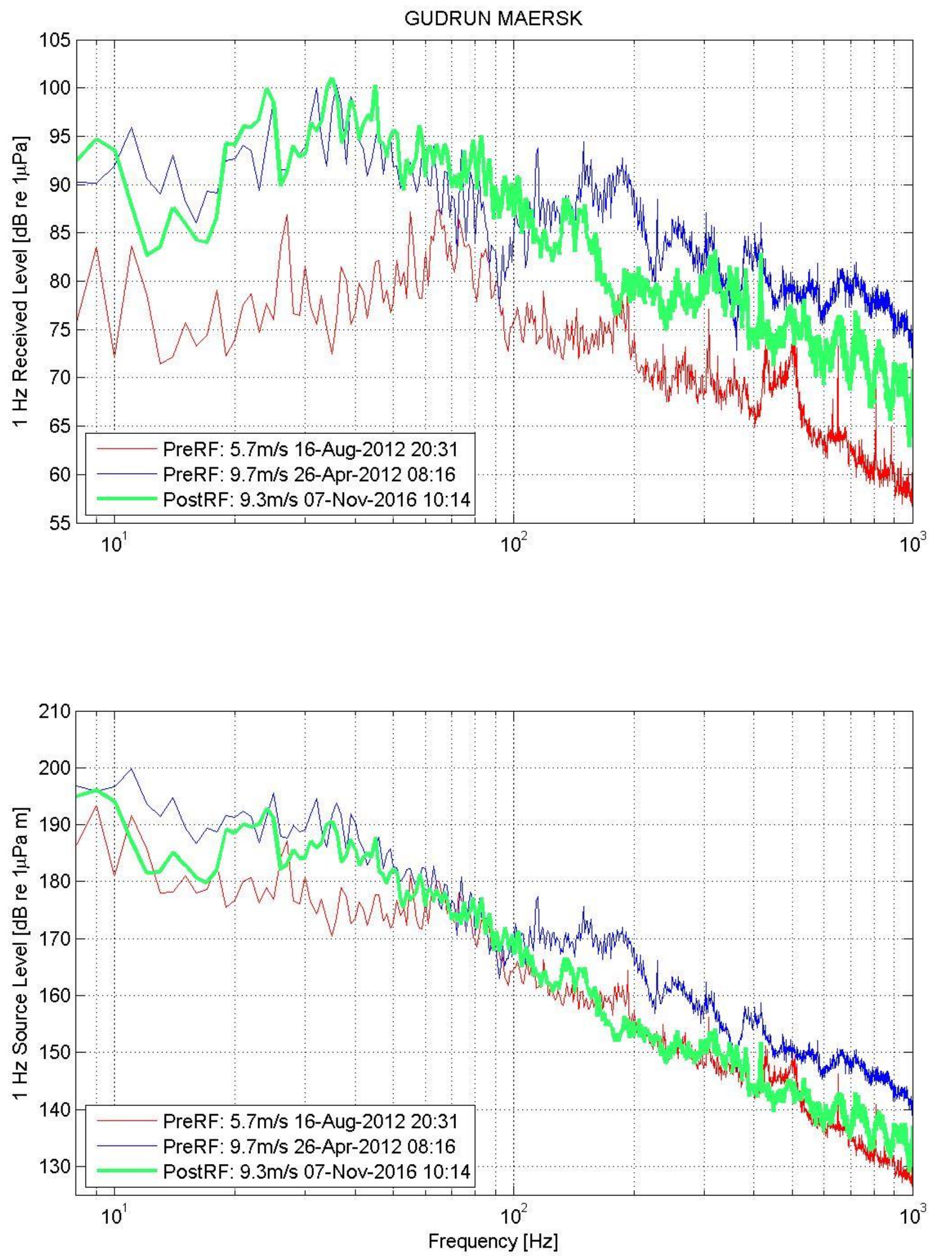

Figure 4 Measured received sound pressure levels at the HARP (upper panel) and estimated source sound pressure levels (lower panel) as a function of frequency for three transits of GUDRUN. Two transits were pre-retrofit at low (5.7 m/s) and high speed (9.7 m/s) (red and blue line respectively). Third transit was post-retrofit at high speed (9.3 m/s) (green line).

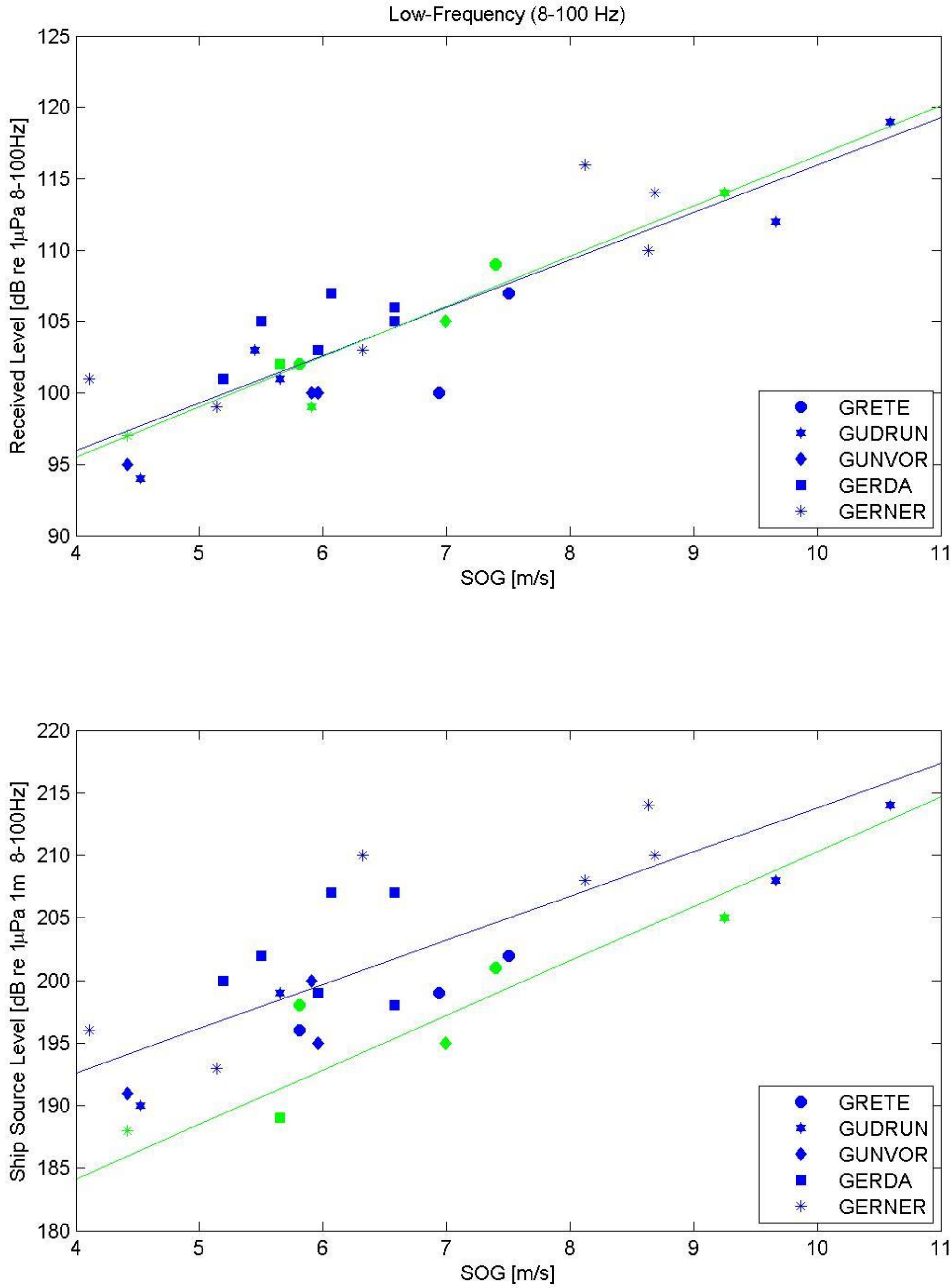

Figure 5 Low-frequency band (8 - 100 Hz) integrated received sound pressure level at HARP (upper panel) and source sound pressure level (lower panel) as a function of speed over ground (SOG) for GRETE (circles), GUDRUN (hexagrans), GUNVOR (diamonds), GERDA (squares) and GERNER (stars). Lines represent polynomials of first order fitted with a Theil-Sen linear regression to the pre- and post-retrofit level distributions. Blue and green color indicates pre- and post-retrofit, respectively.

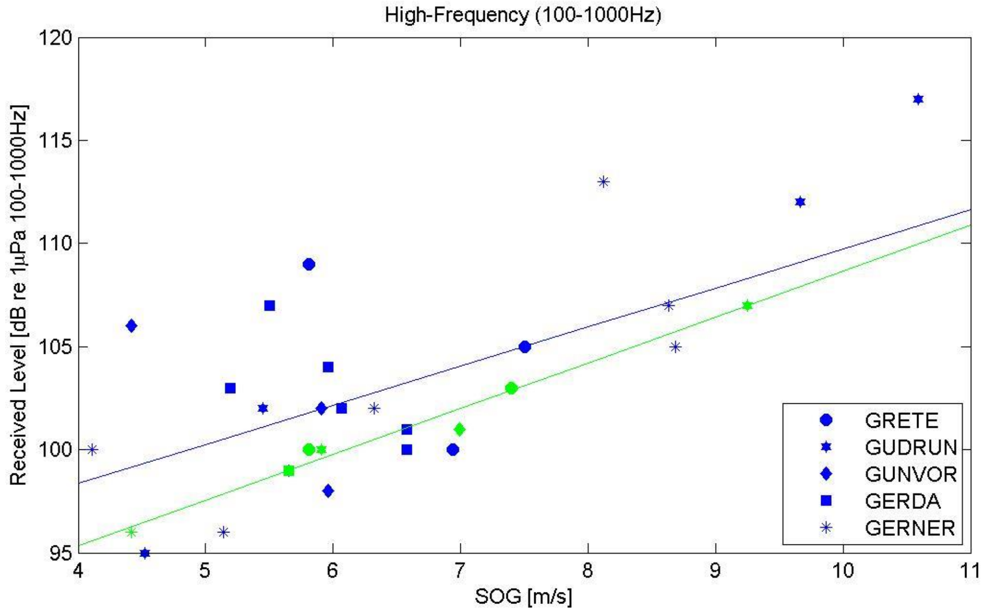

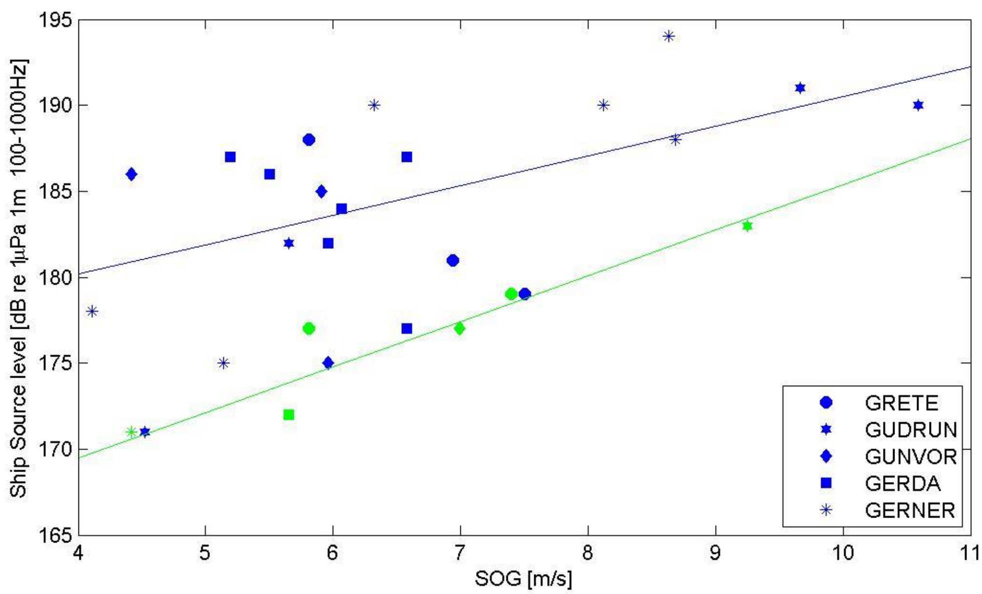

Figure 6 High-frequency band (100 - 1000 Hz) integrated received sound pressure level at HARP (upper panel) and source sound pressure level (lower panel) as a function of speed over ground (SOG) for GRETE (circles), GUDRUN (hexagrans), GUNVOR (diamonds), GERDA (squares) and GERNER (stars) . Lines represent polynomials of first order fitted with a Theil-Sen linear regression to the pre- and post-retrofit level distributions. Blue and green color indicates pre- and post-retrofit, respectively.

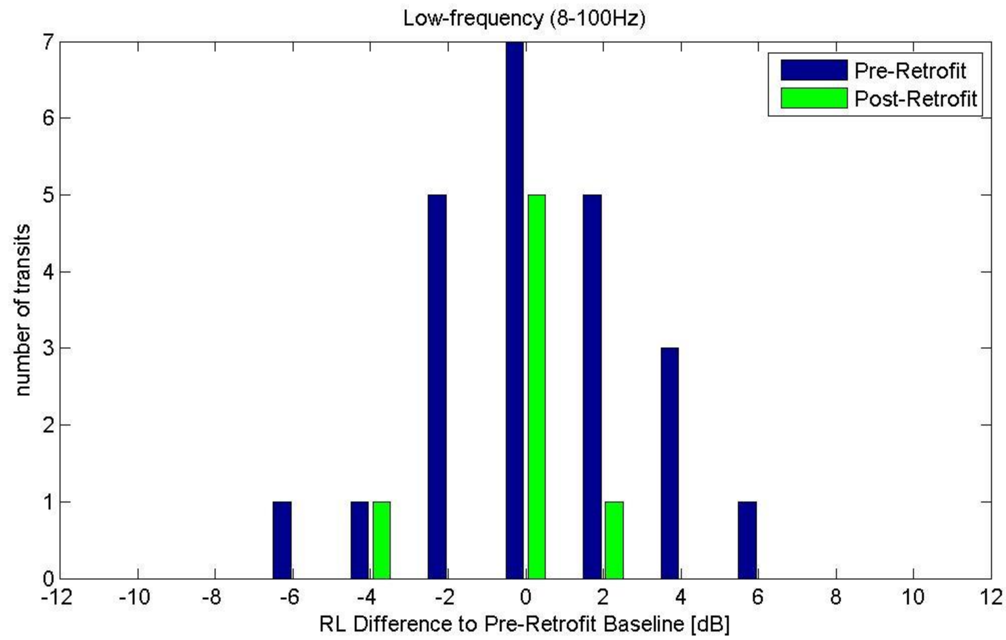

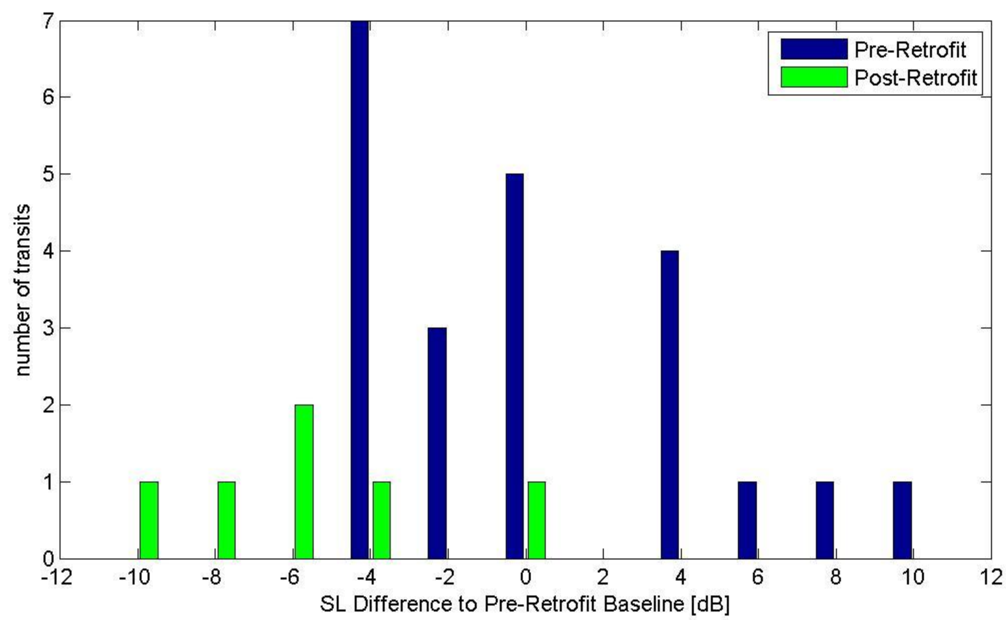

Figure 7 Histogram of differences between post-retrofit levels (green) and pre-retrofit baselines in the low-frequency band (8 – 100 Hz). Upper panel shows differences for received sound pressure levels; lower panel for source sound pressure levels. The goodness of fit for the pre-retrofit baselines (blue lines in Figure 5) is illustrated by the differences between pre-retrofit levels and pre-retrofit base lines in blue.

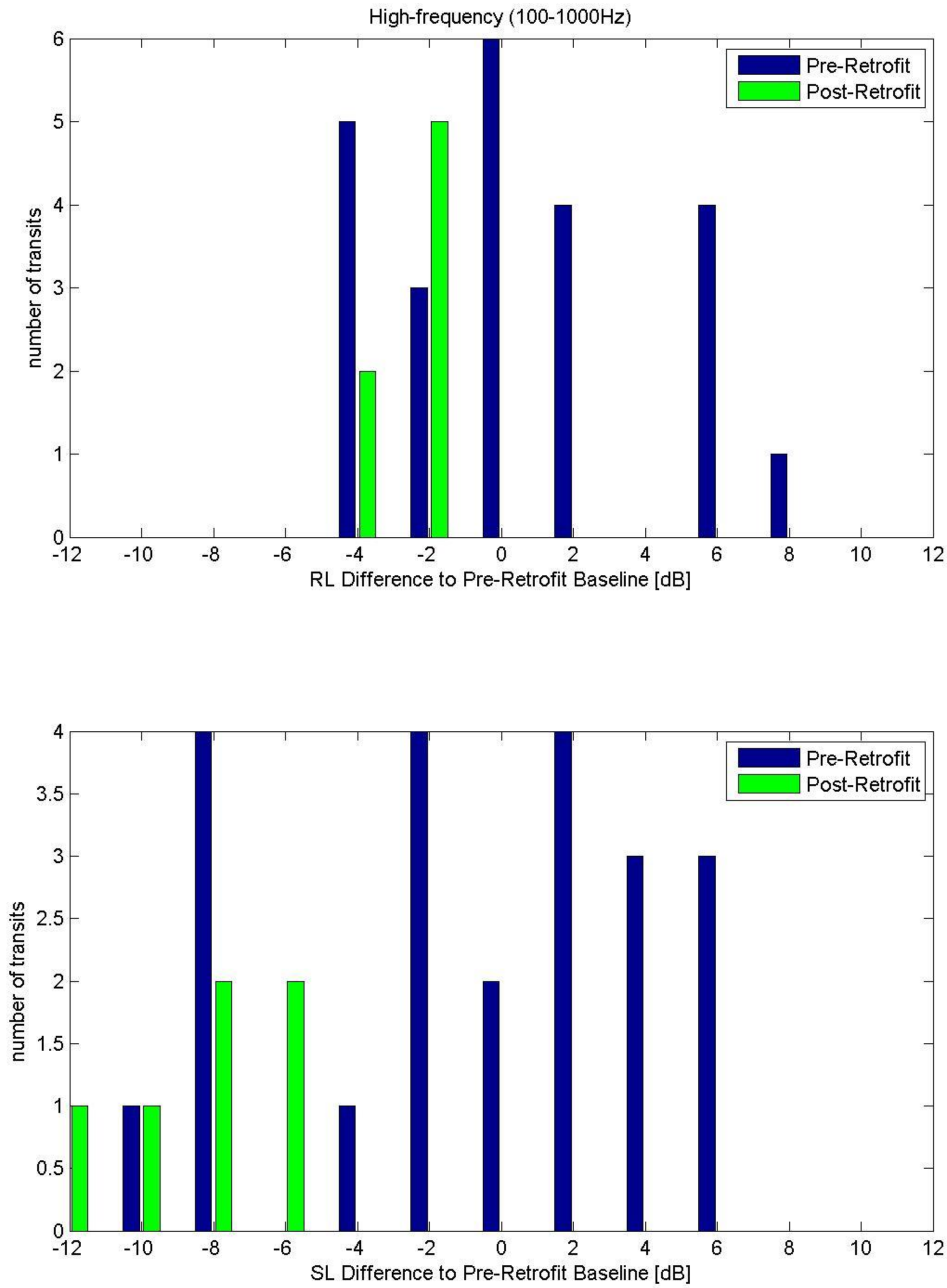

Figure 8 Histogram of differences between post-retrofit levels (green) and pre-retrofit baselines in the high-frequency band (100 – 1000 Hz). Upper panel shows differences for received sound pressure levels; lower panel for source sound pressure levels. The goodness of fit for the pre-retrofit baselines (blue lines in Figure 5) is illustrated by the differences between pre-retrofit levels and pre-retrofit base lines in blue.

Histograms of the differences between the post-retrofit levels and the pre-retrofit baselines are shown in Figure 7 and Figure 8. Reductions in SL of the retrofitted MARSK G-class vessels were 6 and 8 dB for the low- and high-frequency band, respectively. Reductions in RL as measured by the HARP, however, were slightly lower and at a median of 0 and 2 dB for the low- and high-frequency band, respectively, as the reductions in SL were largely compensated by the lower sound transmission loss resulting from the greater draft during the transits of the retrofitted MAERSK G-class vessels.

Discussion and Conclusion

Five container vessels of MAERSK LINE's G-class fleet, GRETE, GUDRUN, GUNVOR, GERDA and GERNER, were selected to compare the underwater noise radiated during a total of 36 opportunistic transits at speeds of 4 – 11 m/s in a shipping lane off the coast of California before and after the vessels' radical retrofit. As the vessels operate at near-surface depths, the Lloyd's mirror effect of reflection from the sea surface must be taken into account to estimate the source sound pressure level of the vessels (Gassmann *et al.*, 2017). The Lloyd's mirror effect involves interference between the source signal and the reflected signal and changes with the depth of the source, that is, the draft of the vessel. Since the draft during the post-retrofit transits examined was up to several meters deeper, less destructive inference is expected. After compensating the Lloyd's mirror effects, the estimated underwater source sound pressure levels of the vessels, were found to be lower after the vessels' retrofit by a median of 6 dB in the low-frequency band (8 - 100 Hz) and a median of 8 dB in the high-frequency band (100 - 1000 Hz). The reduction in source sound pressure levels, in particular in the low-frequency band, may result from less cavitation due to both the retrofitted propellers with boss cap fins, and to propeller operation at greater depth where ambient pressure is higher.

The greater drafts during transits of retrofitted vessels, however, result in smaller sound transmission losses (Lloyd's mirror effect), which largely compensated the reductions in SL of the retrofitted vessels when measured at 3.4 - 5 km distance in 565 m deep water at the location of the acoustic recorder. This effect may be more pronounced at shallower angles lateral to the vessel than at steep angles such as underneath the vessel. Reductions of ship source sound pressure level due to changes such as those employed by the radical retrofits may result in ocean-basin-wide noise reductions.

Acknowledgments

Funding was provided by the Ocean Foundation with support from the National Resources Defense Council and the International Fund for Animal Welfare; we thank Leila Hatch, Michael Jasny, Patrick Ramage, Caroline Coogan and Mark Spaulding. Ryan Griswold, Bruce Thayre, and Erin O'Neill of the Scripps Whale Acoustic Laboratory helped with collecting and archiving the AIS and acoustic data. We thank the captains of the MAERSK G-class fleet for information on vessel draft and Maersk Line Ship Management for other design and performance information.

References

Erbe, C., MacGillivray, A., and Williams, R. (**2012**). "Mapping cumulative noise from shipping to inform marine spatial planning," J. Acoust. Soc. Am. **132**, EL423-EL428.

Gassmann, M., Wiggins, S. M., and Hildebrand, J. A. (**2017**). "Deep-water measurements of container ship radiated noise signatures and directionality," J. Acoust. Soc. Am. **142**, 1563-1574.

Gilbert, R. O. (**1987**). "6.5 Sen's Nonparametric Estimator of Slope," John Wiley and Sons **Statistical Methods for Environmental Pollution Monitoring**, pp. 217–219.

Gray, L. M., and Greeley, D. S. (**1980**). "Source level model for propeller blade rate radiation for the world's merchant fleet," J. Acoust. Soc. Am. **67**, 516-522.

Hildebrand, J. A. (**2009**). "Anthropogenic and natural sources of ambient noise in the ocean," Marine Ecology-Progress Series **395**, 5-20.

Jansen, H. W., and de Jong, C. A. F. (**2015**). "Experimental assessment of underwater radiated sound of different ship types," in *OCEANS 2015 - Genova*, pp. 1-8.

MAERSK LINE (**2017**). "Maersk Ocean-Going Vessel Energy Efficiency Demonstration Project," Technology Advancement Project (TAP) Project Milestone Report.

McKenna, M. F., Katz, S. L., Wiggins, S. M., Ross, D., and Hildebrand, J. A. (**2012a**). "A quieting ocean: Unintended consequence of a fluctuating economy," J. Acoust. Soc. Am. **132**, EL169-EL175.

McKenna, M. F., Ross, D., Wiggins, S. M., and Hildebrand, J. A. (**2012b**). "Underwater radiated noise from modern commercial ships," J. Acoust. Soc. Am. **131**, 92-103.

McKenna, M. F., Wiggins, S. M., and Hildebrand, J. A. (**2013**). "Relationship between container ship underwater noise levels and ship design, operational and oceanographic conditions," Scientific Reports **3**, 1760.

Redfern, J. V., Hatch, L. T., Caldow, C., DeAngelis, M. L., Gedamke, J., Hastings, S., Henderson, L., McKenna, M. F., Moore, T. J., and Porter, M. B. (**2017**). "Assessing the risk of chronic shipping noise to baleen whales off Southern California, USA," Endangered Species Research **32**, 153-167.

Ross, D. (**1976**). "Mechanics of underwater noise," (Pergamon Press, New York).

Simard, Y., Roy, N., Gervaise, C., and Giard, S. (**2016**). "Analysis and modeling of 255 source levels of merchant ships from an acoustic observatory along St. Lawrence Seaway," J. Acoust. Soc. Am. **140**, 2002-2018.

UNCTAD (**2016**). "Review of Maritime Transport," http://unctad.org/en/PublicationsLibrary/rmt2016_en.pdf.

Urick, R. J. (**1975**). *Principles of Underwater Sound* (McGraw-Hill, New York).

Webb, S. C. (**1998**). "Broadband seismology and noise under the ocean," Reviews of Geophysics **36**, 105-142.

Wenz, G. M. (**1962**). "Acoustic ambient noise in the ocean: spectra and sources," J Acoustic Soc Am **34**, 1936-1956.

Wiggins, S. M., and Hildebrand, J. A. (**2007**). "High-frequency Acoustic Recording Package (HARP) for broad-band, long-term marine mammal monitoring," in *International Symposium on Underwater Technology 2007 and International Workshop on Scientific Use of Submarine Cables & Related Technologies 2007* (Institute of Electrical and Electronics Engineers, Tokyo, Japan), pp. 551-557.

Appendix A

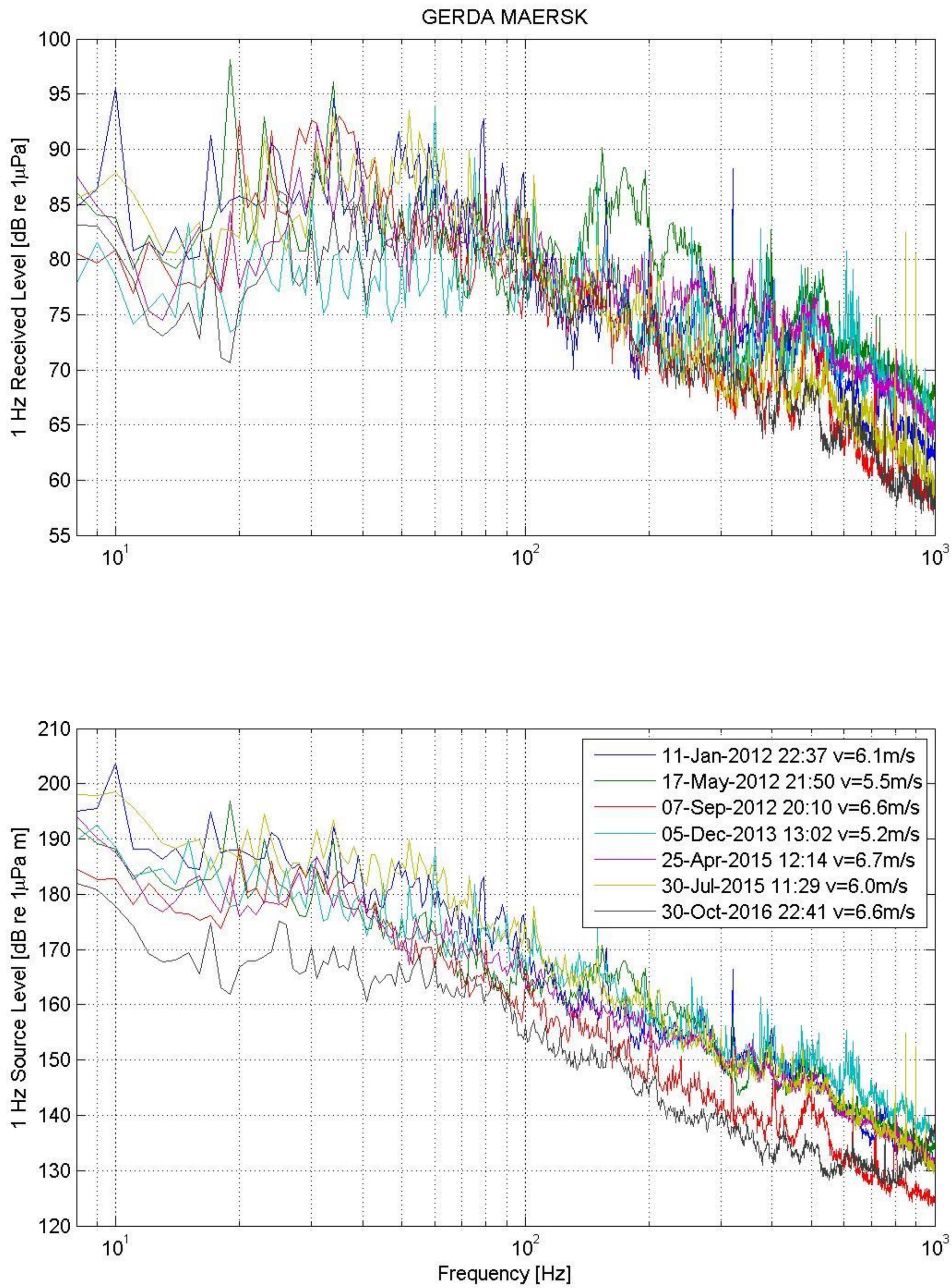
GERDA MAERSK
1 Hz Received Level [dB re 1μPa]
11-Jan-2012 22:37 v=6.1m/s
17-May-2012 21:50 v=5.5m/s
07-Sep-2012 20:10 v=6.6m/s
05-Dec-2013 13:02 v=5.2m/s
25-Apr-2015 12:14 v=6.7m/s
30-Jul-2015 11:29 v=6.0m/s
30-Oct-2016 22:41 v=6.6m/s
1 Hz Source Level [dB re 1μPa m]
Frequency [Hz]

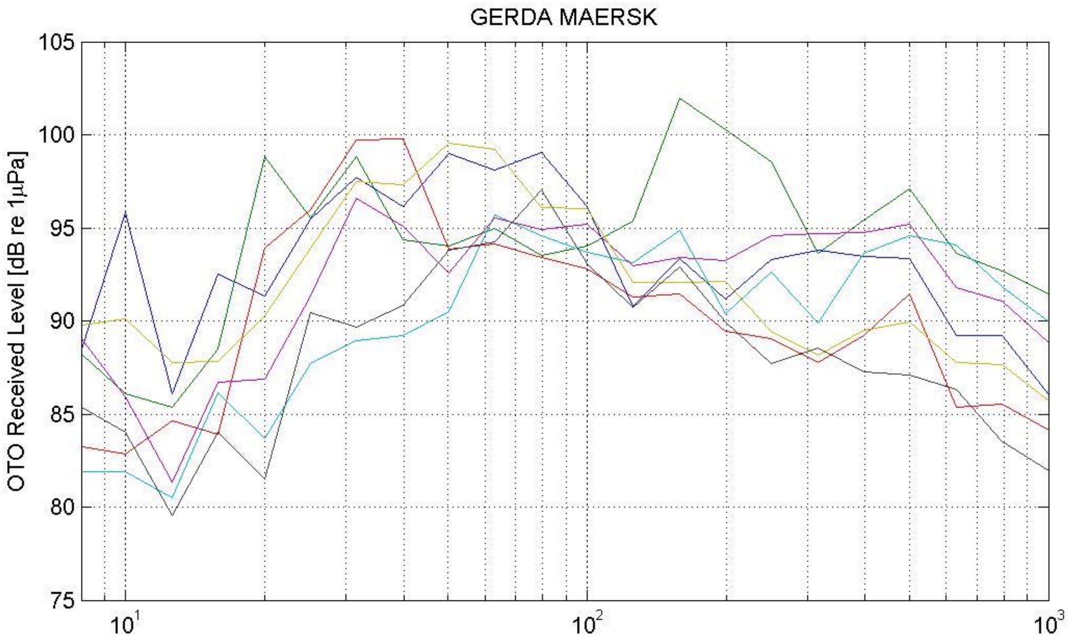

GERDA MAERSK
OTO Received Level [dB re 1μPa]
105
100
95
90
85
80
75
10^1
10^2
10^3

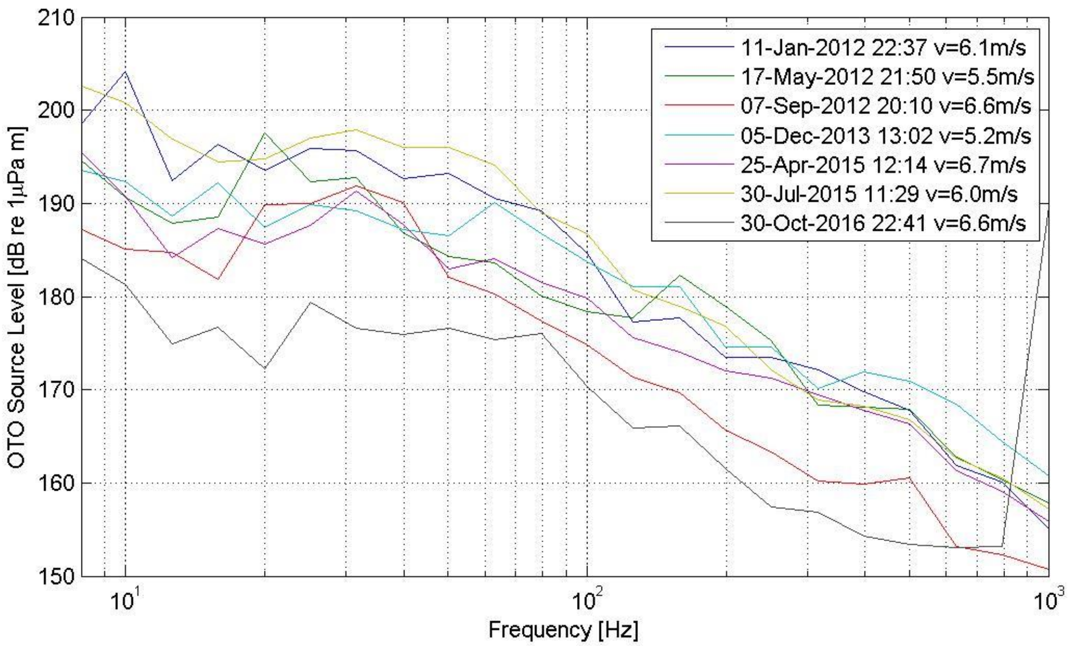

OTO Source Level [dB re 1μPa m]
210
200
190
180
170
160
150
10^1
10^2
10^3
Frequency [Hz]
11-Jan-2012 22:37 v=6.1m/s
17-May-2012 21:50 v=5.5m/s
07-Sep-2012 20:10 v=6.6m/s
05-Dec-2013 13:02 v=5.2m/s
25-Apr-2015 12:14 v=6.7m/s
30-Jul-2015 11:29 v=6.0m/s
30-Oct-2016 22:41 v=6.6m/s

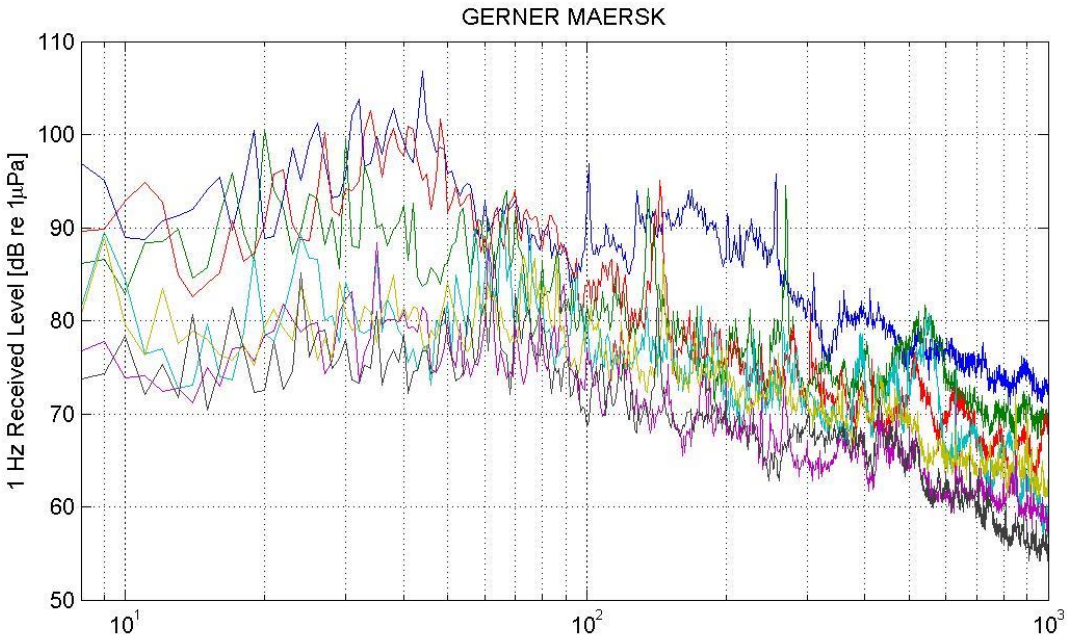
GERNER MAERSK
1 Hz Received Level [dB re 1μPa]
110
100
90
80
70
60
50
10^1
10^2
10^3

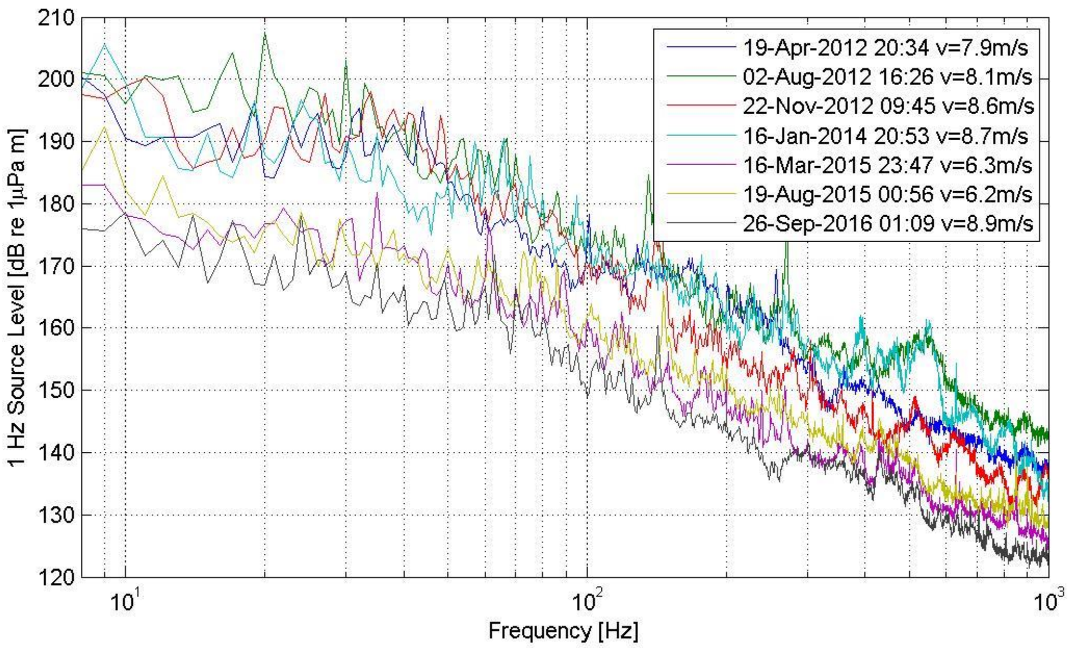
1 Hz Source Level [dB re 1μPa m]
210
200
190
180
170
160
150
140
130
120
10^1
10^2
10^3
Frequency [Hz]
19-Apr-2012 20:34 v=7.9m/s
02-Aug-2012 16:26 v=8.1m/s
22-Nov-2012 09:45 v=8.6m/s
16-Jan-2014 20:53 v=8.7m/s
16-Mar-2015 23:47 v=6.3m/s
19-Aug-2015 00:56 v=6.2m/s
26-Sep-2016 01:09 v=8.9m/s

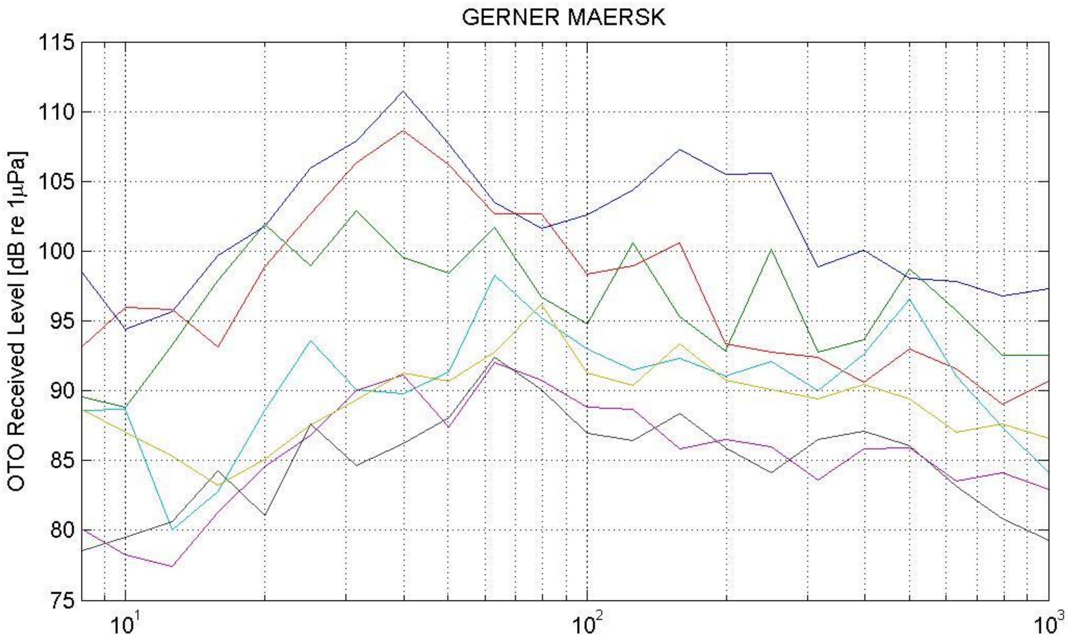

GERNER MAERSK
OTO Received Level [dB re 1μPa]
115
110
105
100
95
90
85
80
75
10^1
10^2
10^3

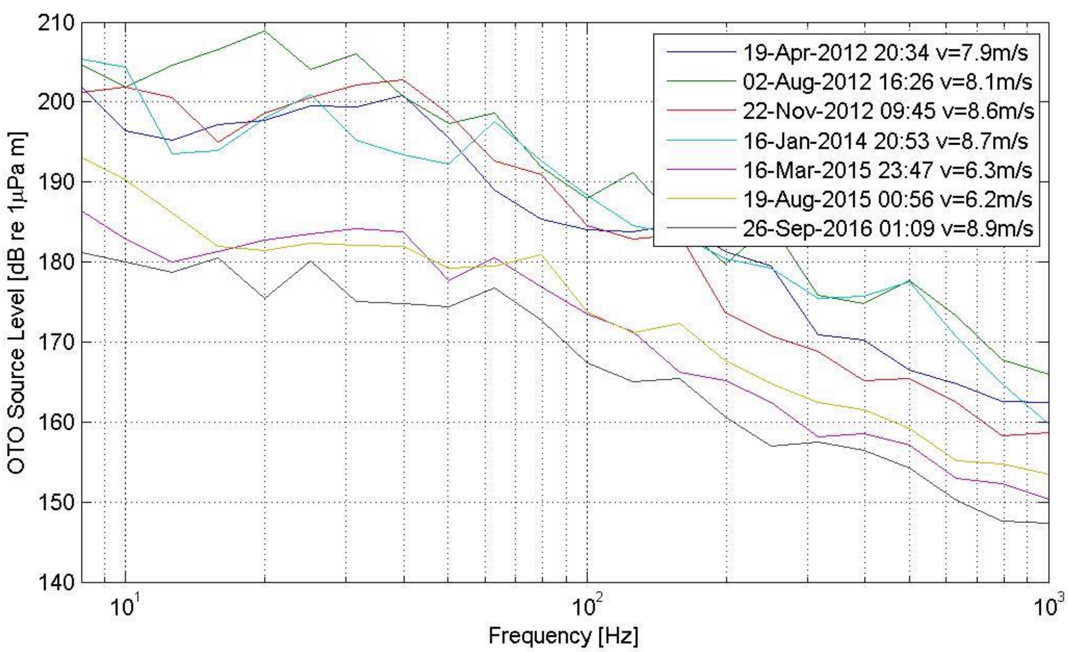

OTO Source Level [dB re 1μPa m]
210
200
190
180
170
160
150
140
10^1
10^2
10^3
Frequency [Hz]
19-Apr-2012 20:34 v=7.9m/s
02-Aug-2012 16:26 v=8.1m/s
22-Nov-2012 09:45 v=8.6m/s
16-Jan-2014 20:53 v=8.7m/s
16-Mar-2015 23:47 v=6.3m/s
19-Aug-2015 00:56 v=6.2m/s
26-Sep-2016 01:09 v=8.9m/s

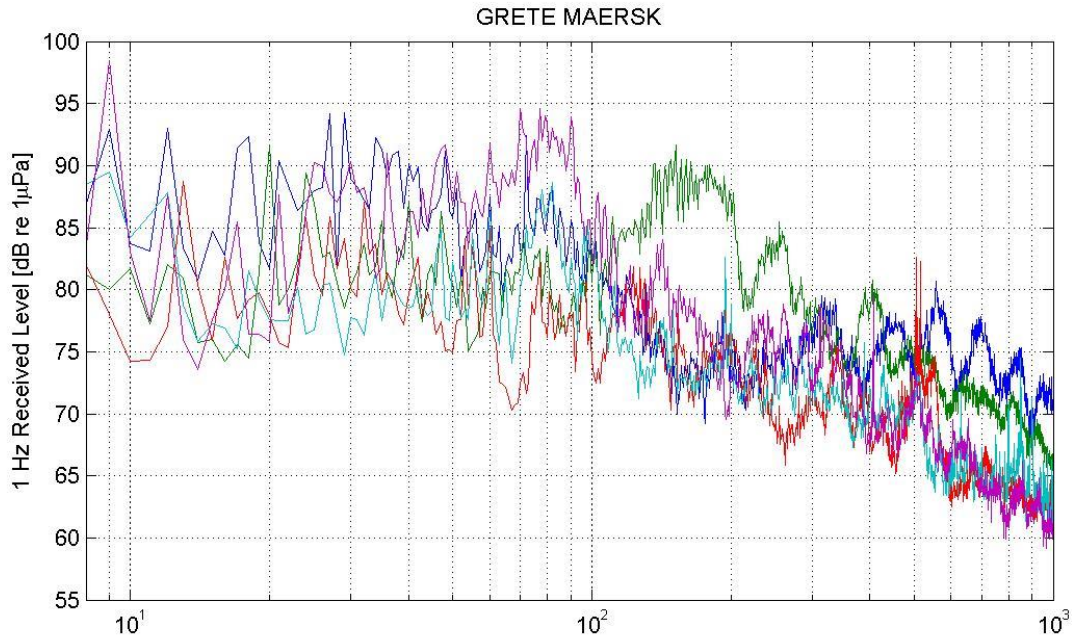
GRETE MAERSK
1 Hz Received Level [dB re 1μPa]
100
95
90
85
80
75
70
65
60
55
10^1
10^2
10^3

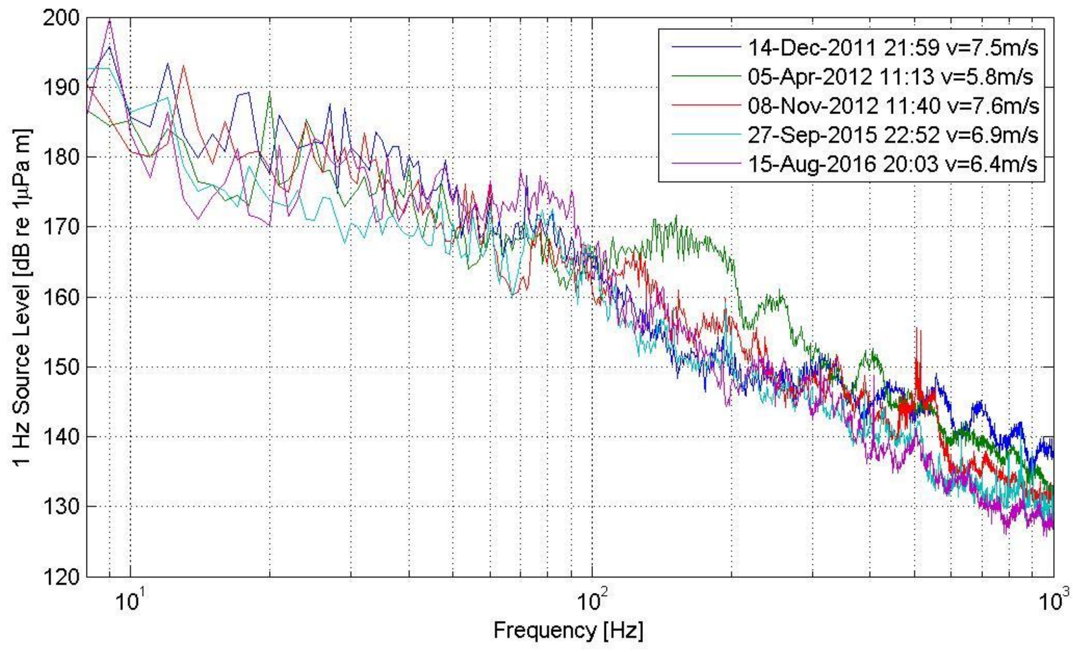
14-Dec-2011 21:59 v=7.5m/s
05-Apr-2012 11:13 v=5.8m/s
08-Nov-2012 11:40 v=7.6m/s
27-Sep-2015 22:52 v=6.9m/s
15-Aug-2016 20:03 v=6.4m/s
1 Hz Source Level [dB re 1μPa m]
200
190
180
170
160
150
140
130
120
10^1
10^2
10^3
Frequency [Hz]

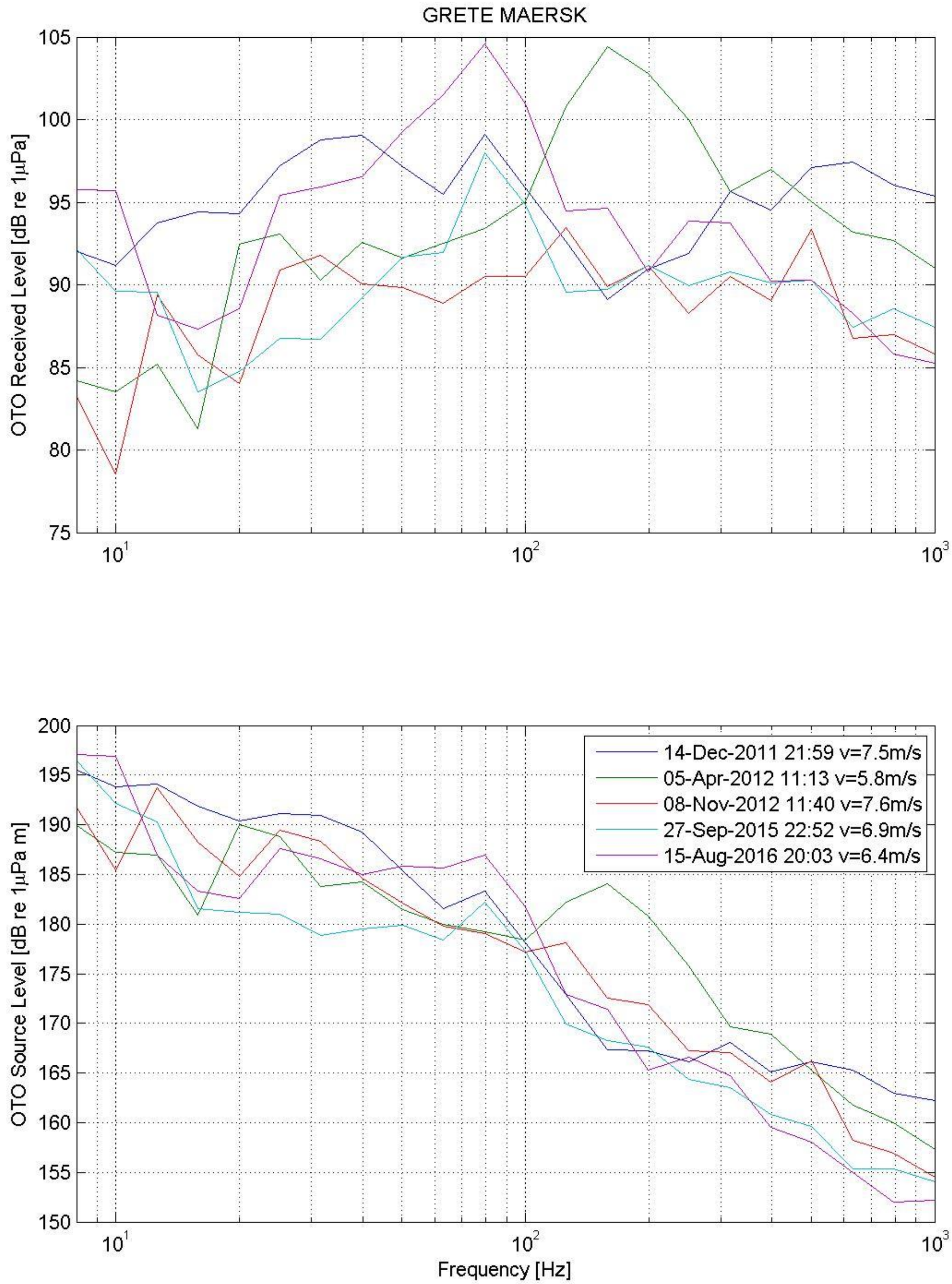
GRETE MAERSK
OTO Received Level [dB re 1μPa]
OTO Source Level [dB re 1μPa m]
Frequency [Hz]
14-Dec-2011 21:59 v=7.5m/s
05-Apr-2012 11:13 v=5.8m/s
08-Nov-2012 11:40 v=7.6m/s
27-Sep-2015 22:52 v=6.9m/s
15-Aug-2016 20:03 v=6.4m/s

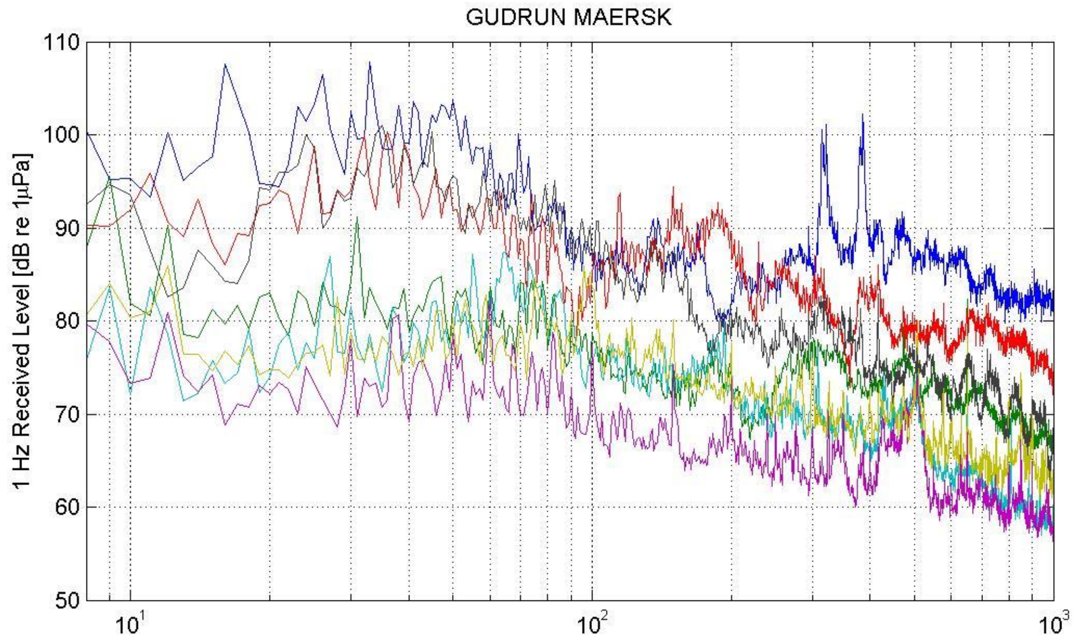
GUDRUN MAERSK
1 Hz Received Level [dB re 1μPa]
110
100
90
80
70
60
50
10^1
10^2
10^3

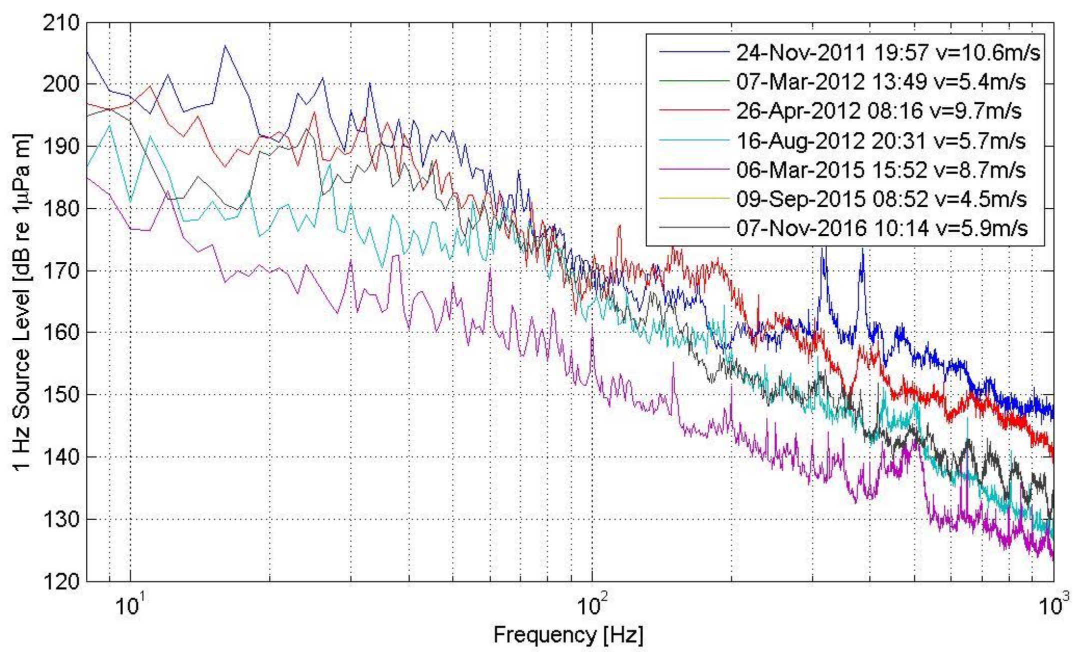
1 Hz Source Level [dB re 1μPa m]
210
200
190
180
170
160
150
140
130
120
10^1
10^2
10^3
Frequency [Hz]
24-Nov-2011 19:57 v=10.6m/s
07-Mar-2012 13:49 v=5.4m/s
26-Apr-2012 08:16 v=9.7m/s
16-Aug-2012 20:31 v=5.7m/s
06-Mar-2015 15:52 v=8.7m/s
09-Sep-2015 08:52 v=4.5m/s
07-Nov-2016 10:14 v=5.9m/s

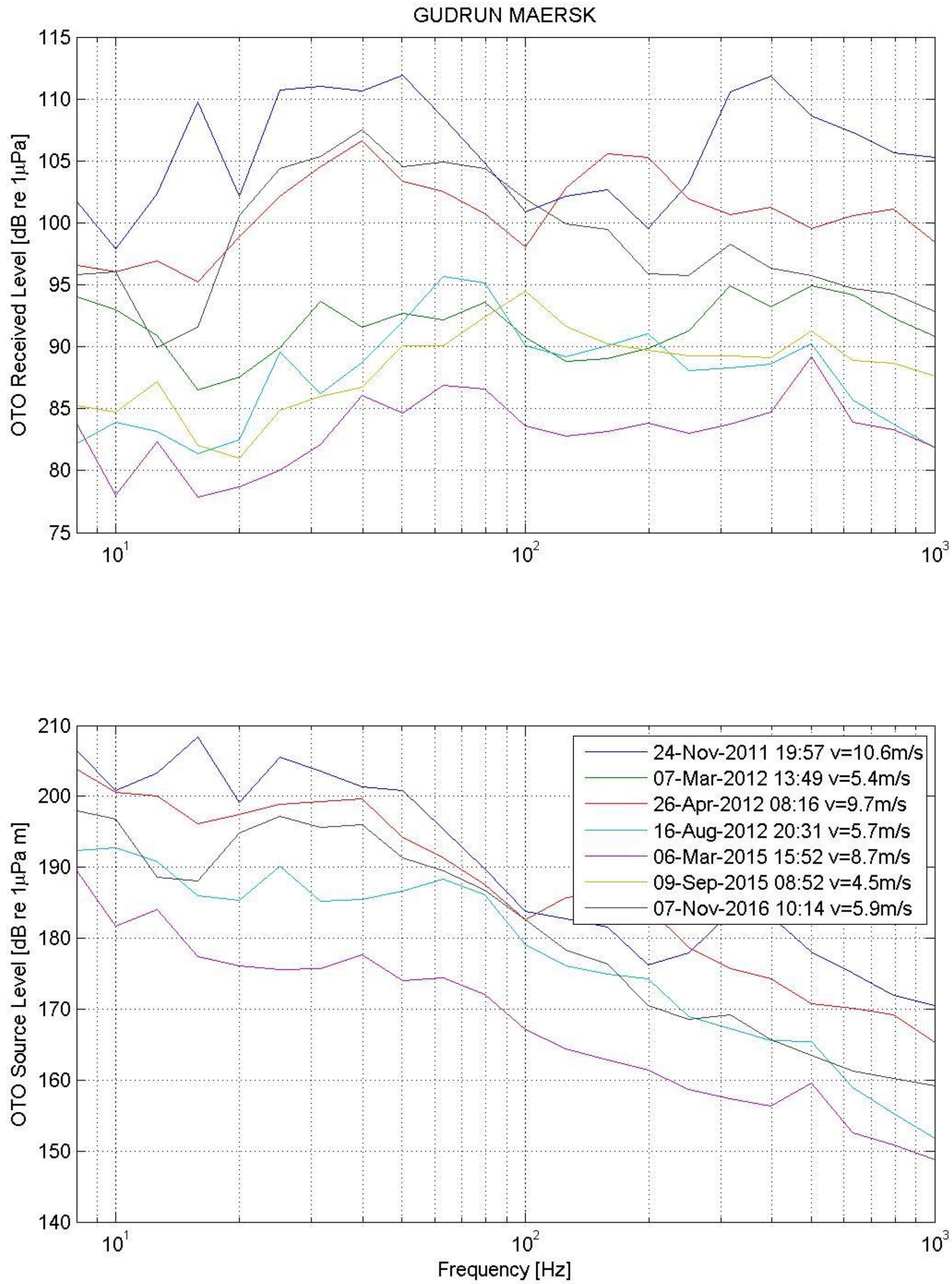
GUDRUN MAERSK
OTO Received Level [dB re 1μPa]
OTO Source Level [dB re 1μPa m]
Frequency [Hz]
24-Nov-2011 19:57 v=10.6m/s
07-Mar-2012 13:49 v=5.4m/s
26-Apr-2012 08:16 v=9.7m/s
16-Aug-2012 20:31 v=5.7m/s
06-Mar-2015 15:52 v=8.7m/s
09-Sep-2015 08:52 v=4.5m/s
07-Nov-2016 10:14 v=5.9m/s

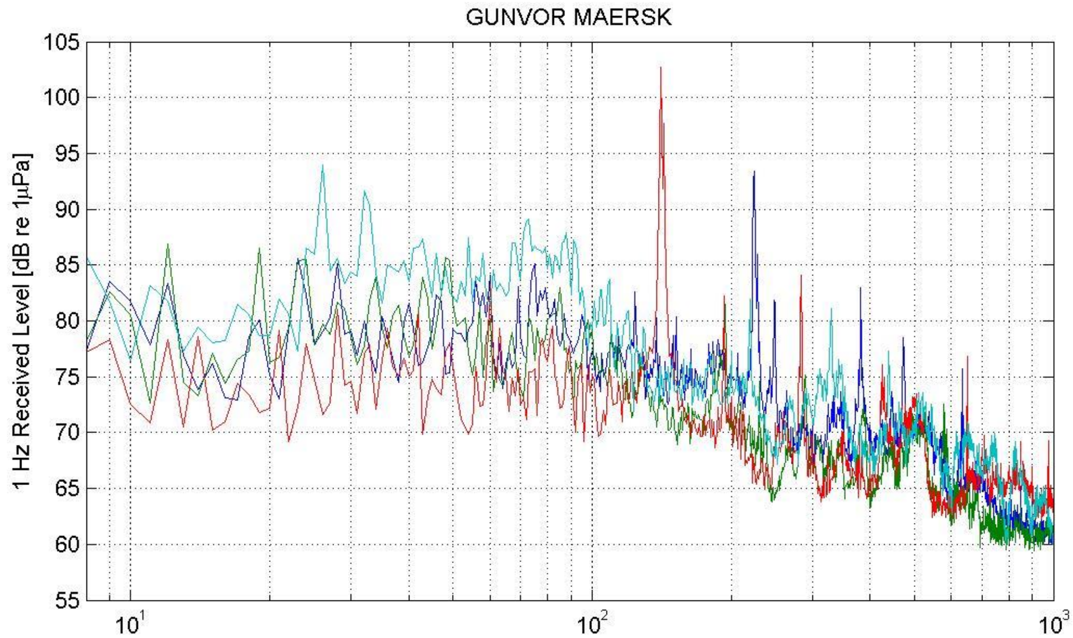
GUNVOR MAERSK
1 Hz Received Level [dB re 1μPa]
105
100
95
90
85
80
75
70
65
60
55
10^1
10^2
10^3

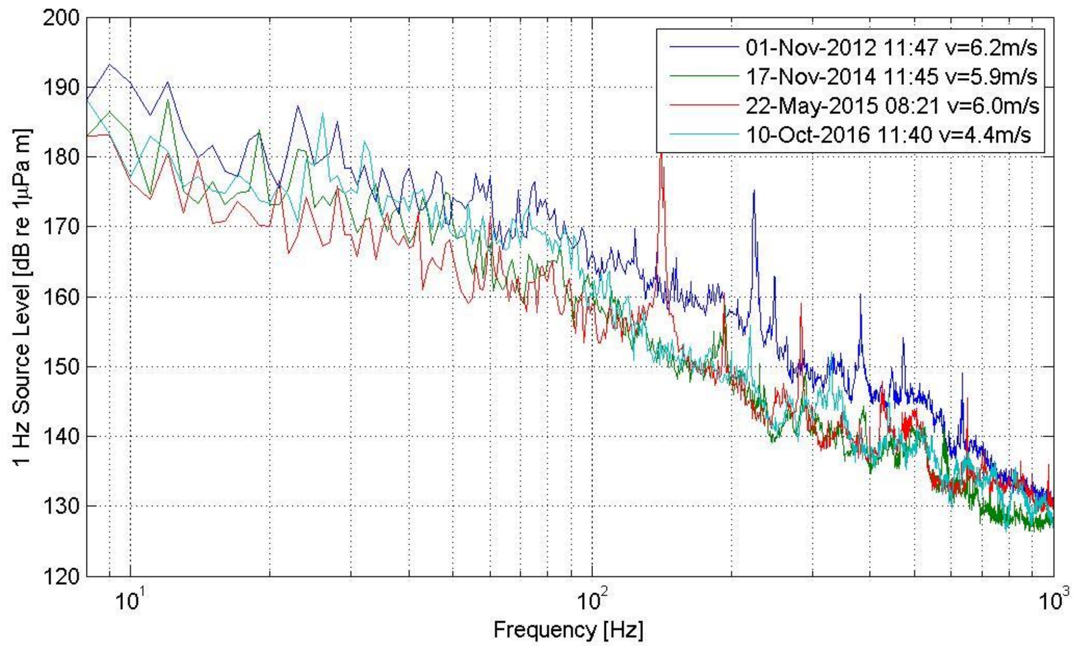
1 Hz Source Level [dB re 1μPa m]
01-Nov-2012 11:47 v=6.2m/s
17-Nov-2014 11:45 v=5.9m/s
22-May-2015 08:21 v=6.0m/s
10-Oct-2016 11:40 v=4.4m/s
200
190
180
170
160
150
140
130
120
10^1
10^2
10^3
Frequency [Hz]

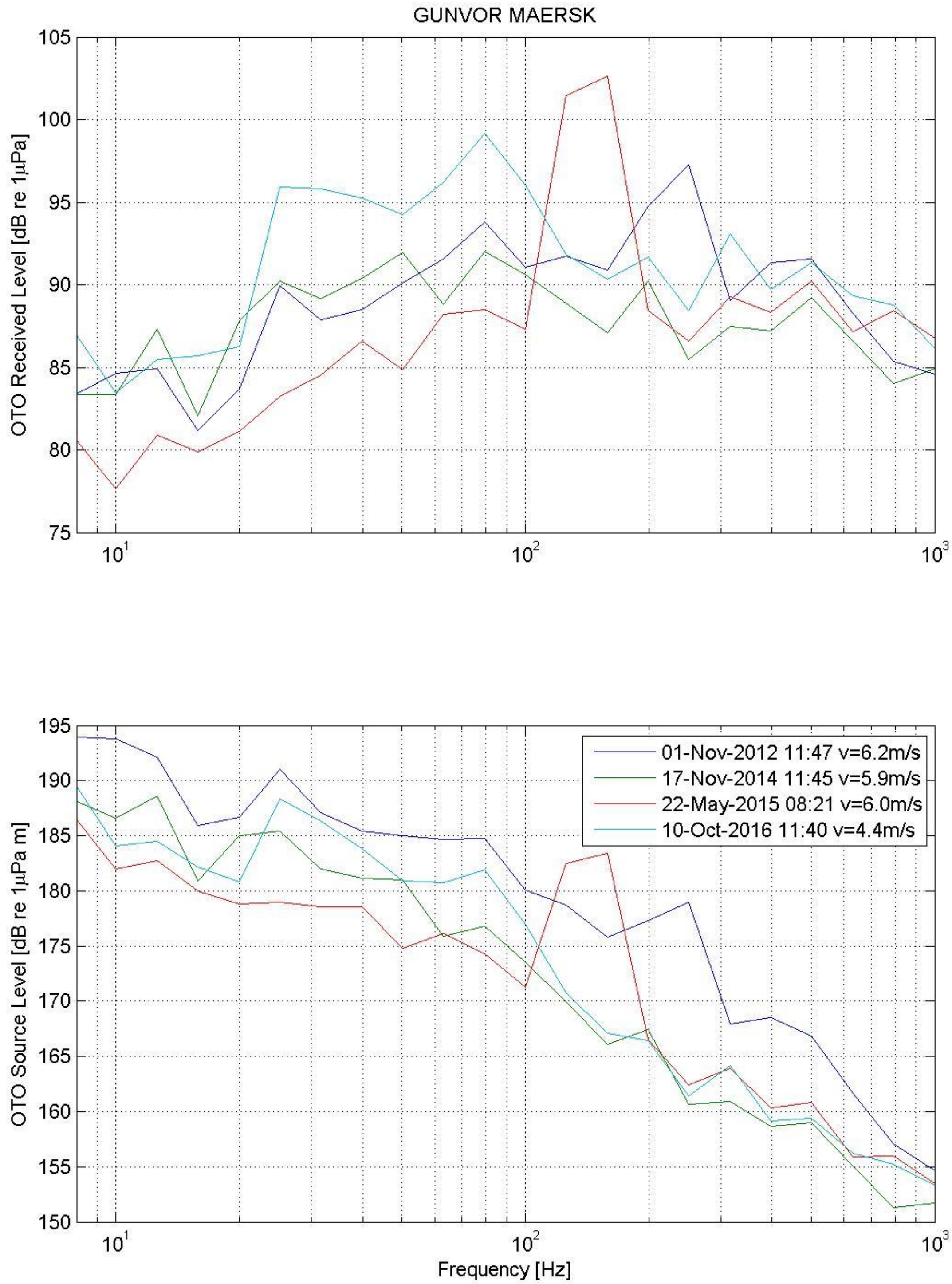

GUNVOR MAERSK
OTO Received Level [dB re 1μPa]
OTO Source Level [dB re 1μPa m]
Frequency [Hz]
01-Nov-2012 11:47 v=6.2m/s
17-Nov-2014 11:45 v=5.9m/s
22-May-2015 08:21 v=6.0m/s
10-Oct-2016 11:40 v=4.4m/s